

Water hydrogen-bond dynamics close to hydrophobic and hydrophilic groups

Alenka Luzar

Department of Chemistry, University of California, Berkeley, California 94720-1460, USA

We discuss the analysis of molecular dynamics calculations where we simulate the kinetics of the breaking and forming of hydrogen bonds in distinctly different environments: liquid water and concentrated aqueous solution of DMSO. In our analysis, we consider reactive flux correlation functions computed for a variety of specific conditions and identify rate constants for bond making and breaking in terms of the liquid's molecular dynamics. According to the proposed mechanism of hydrogen-bond kinetics, hydrogen bonds most frequently break during a process of switching allegiance with a newly formed bond replacing the broken one. Simulations reveal bond dynamics in the mixture to be significantly slower than in pure water. This is interpreted in terms of reduced likelihood of fluctuations in the hydrogen-bond network, related to the presence of free hydrogen-bonding sites, which participate in the process of switching allegiances. Implications of our analysis for future experimental work are briefly discussed.

1 Introduction

The dynamics of hydration in aqueous solutions involves the making and breaking of hydrogen bonds. We have studied the statistical evolution of these processes. The elemental process of the breaking and forming of hydrogen bonds in liquids has been probed indirectly through a variety of experimental techniques.¹ Although typically limited to classical models, the method of molecular dynamics is a powerful tool to obtain a more direct microscopic picture of hydrogen-bond dynamics in molecular liquids.² Factors controlling the dynamics can be determined from trajectory calculations of correlation functions.³ Analysis of computer generated Newtonian trajectories in liquid water reveal long time non-exponential kinetics of hydrogen bonds.^{4–6} The relaxation of hydrogen bonds in water therefore appears very complicated, with no simple characterization in terms of a few relaxation times or rate constants. Most of the speculations about this apparently complicated kinetics pointed to cooperativity between neighbouring hydrogen bonds as the source of the complexity.⁷ Our recent work⁵ demonstrates that the mechanism lies elsewhere, with virtually self evident coupling that exists between translational diffusion and hydrogen-bond dynamics. Diffusion governs whether a specific pair of water molecules are near-neighbours. Hydrogen bonds between such adjacent pairs form and persist at random, with average lifetimes determined by rate constants for bond making and breaking.

In this paper, our model and analysis⁵ is applied to study the hydrogen-bond dynamics in the hydration process of dimethyl sulphoxide (DMSO). DMSO is a solute that is miscible in all proportions and forms strong hydrogen bonds with water, but also has methyl groups which do not form associative bonds. The water–DMSO mixture therefore provides a simple molecular model for studying competing effects of hydro-

phobicity and hydrophilicity on hydrogen-bond kinetics. An analysis of computed and experimental distribution functions revealed an enhancement of water–water hydrogen-bond correlations in the presence of hydrophobic and hydrophilic groups on DMSO.^{8,9} The timescales associated with these correlations are examined in Section 3. Recently performed computer simulations, presented here for the first time, show that on long timescales the relaxation behaviour of hydrogen bonds in the concentrated aqueous solutions of DMSO exhibit the analogous non-exponential kinetics, as was observed in pure water. Adopting the same analysis as for pure water, we determine rate constants for breaking and making of water–water and water–DMSO hydrogen bonds in the mixture in the same section. First, however, the methods of the analysis, and the application to the hydrogen-bond kinetics in pure liquid water are outlined in Section 2.

2 Hydrogen-bond kinetics in liquid water

We studied the time dependence of hydrogen-bond dynamics in liquid water using computer simulations.^{5,6} In particular, we performed molecular dynamics computations of hydrogen-bond population correlation functions and a variety of configuration specific reactive flux correlation functions. In the following, we describe basic methods and definitions introduced in this analysis.

2.1 Reactive flux correlation functions and rate constants

Let us first briefly sketch the correlation function formalism for the calculation of the rate constants of chemical reactions in solution (in this case hydrogen-bond making and breaking), treated in the framework of classical statistical mechanics.

According to a configurational criterion for whether a particular pair of molecules is hydrogen bonded, we can define a hydrogen-bond population operator, h . It is unity if the particular tagged pair of molecules is hydrogen bonded, according to the adopted definition,^{8,10} and is zero otherwise.

The average number of hydrogen bonds in an equilibrium of N water molecules is $\frac{1}{2}N(N-1)\langle h \rangle$, where $\langle h \rangle$ denotes the time average of h . In the dynamical equilibrium, h fluctuates in time. These fluctuations are characterized by the hydrogen-bond correlation function, $c(t)$:

$$c(t) = \langle h(0)h(t) \rangle / \langle h \rangle \quad (1)$$

where the angular brackets indicate the ensemble average over initial times. $c(t)$ denotes the probability that the hydrogen bond is intact at time t , given it was intact at time zero. At equilibrium, the probability that a specific pair of molecules is bonded in a large system is negligibly small. $c(t)$ therefore relaxes to zero. According to the fluctuation–dissipation theorem (or equivalently, Onsager’s regression hypothesis),¹¹ the time evolution of $c(t)$ is the same as that for an initially prepared non-equilibrium concentration of hydrogen bonds.

The rate of relaxation to equilibrium is characterized by the reactive flux correlation function, $k(t)$:

$$k(t) = -dc/dt = \langle j(0)[1 - h(t)] \rangle / \langle h \rangle \quad (2)$$

where $j(0) = -dh/dt|_{t=0}$ is the integrated flux departing the hydrogen-bond configuration space at time zero. The function $k(t)$ is the average of this integrated flux for those trajectories where the bond is broken at a time t later, hence the terminology ‘reactive flux’. Its zero time value is the statistical transition-state theory (TST) approximation to the rate constant, k_{TST} .^{12,13}

Dynamical corrections to the TST estimate of the rate constant are conveniently expressed in terms of the transmission coefficient κ , which relates the classical TST

expression¹⁴ to the exact forward-rate constant:¹²

$$k = \kappa k_{\text{TST}} \quad (3)$$

Roughly speaking, κ is the fraction of successful or undeterred activated trajectories.

For the simplest dynamical process, functions like $k(t)$ will settle to a plateau value after an initial transient relaxation period. This plateau value would then determine the rate constant, k , for the process. The existence of a well defined plateau in time would imply a linear rate law.^{12,15} That is, if $k(t)$ exhibited a plateau value k , then at times long compared with the initial decay, $k(t) \approx k \exp(-kt)$, with $1/k$ corresponding to the average hydrogen-bond lifetime.

It is evident, however, from our calculations (Fig. 1) that $k(t)$ does not relax exponentially. Beyond the transient period of *ca.* 0.2 ps, which corresponds to librations on a timescale of less than 0.1 ps, and inter-oxygen vibrations on a timescale of 0.1–0.2 ps, the slope of $\log k(t)$ increases monotonically with time.⁵ Note that the behaviour of $k(t)$ beyond the short time transient period is invariant to physically reasonable changes in hydrogen-bond definition.^{5,6}

We,¹⁸ as many others,⁷ have speculated that the source of non-exponential kinetics of tagged hydrogen bonds in water is due to correlations between different hydrogen bonds. We explored this possibility in detail by partitioning the trajectories that contribute to the reactive flux according to the particular environment of the hydrogen bond.⁶ These calculations unambiguously show that what happens to the dynamics at the transition state and beyond is to a good approximation uncorrelated with the initial bonding state. Lack of correlations between the dynamics of a tagged hydrogen bond

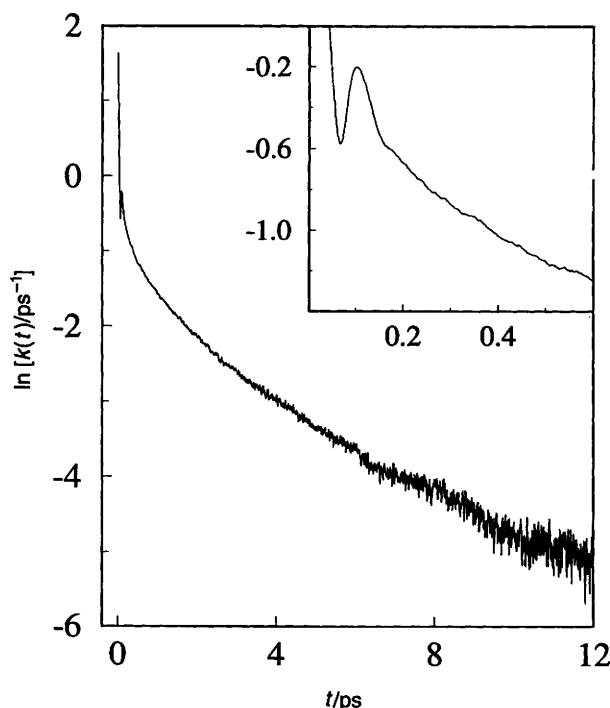


Fig. 1 Reactive flux correlation functions, $k(t)$, for water at room temperature, and density 1 g cm⁻³, sampled over 240 ps of physical time. SPC¹⁶ potential model was employed, using periodic boundary conditions and Ewald sums.¹⁷ The inset panel shows the portion of the trajectory, from which k and k' were evaluated according to eqn. (7).

and that of its neighbours should lead to a single relaxation time and therefore these dynamics should be characterized by well defined rate constants. And indeed, rate constants do exist, although the rate function $k(t)$ clearly exhibits non-exponential kinetics. The reason for this apparent inconsistency has to do with diffusion. Because of diffusion, recrossings in and out of the hydrogen-bond configuration space never stop and these recrossings affect $k(t)$ at all times.

The source of significant non-exponential relaxation for water at ambient conditions is therefore the coupling between hydrogen-bond population and diffusion.⁵ In particular, two molecules can diffuse apart only after the hydrogen bond between them breaks, and a broken bond can reform if a molecule reverses its direction and diffuses back to its partner. This aspect of hydrogen-bond dynamics introduces a continuum of relaxation times. Quantitative consequences of diffusion were examined by partitioning the contributors to $k(t)$ according to whether or not a pair has moved apart after its bond has broken. From this partitioning we have computed a restricted reactive flux function, $k_{\text{in}}(t)$:

$$k_{\text{in}}(t) = \langle j(0)[1 - h(t)]H(t) \rangle / \langle h \rangle \quad (4)$$

where $H(t)$ is unity if the oxygen–oxygen distance of the tagged pair is not larger than $R_{\text{OO}}^{(c)}$ (Table 1) and it is zero otherwise. The probability at time t that a pair of initially bonded molecules are now unbonded but remain separated by less than $R_{\text{OO}}^{(c)}$, is evaluated by $n(t)$:

$$n(t) = \int_0^t dt' k_{\text{in}}(t') \quad (5)$$

The time dependence of this population shows (Fig. 2) that there is quite a significant amount of bonds that break, but the molecules that previously had a common bond remain nearest neighbours.

The probabilities $c(t)$ and $n(t)$ correspond to local populations that can interconvert. The simplest possible kinetics of this interconversion in the first coordination shell of water molecules is:

$$dc/dt = -kc(t) + k'n(t) \quad (6)$$

where k and k' are the respective rate constants for the breaking and making of hydrogen bonds between a near-neighbour pair of molecules. As the interconversions described by eqn. (6) exclude significant translations, they therefore involve molecular rotations. At very short times translational diffusion does not play a significant role. Therefore we can extract the rate constants from the small time limit of eqn. (6). The only instantaneous contribution to $n(t)$ is the breaking of the bond. Diffusion occurs one step later in time. Hence, the rate of change of $dn/dt|_{t=0}$ is equal to the rate of change of hydrogen-bond breaking, k . Determining the slope of $k(t)$ at time zero and its value at time zero by taking into account the boundary conditions, $c(0) = 1$ and $n(0) = 0$, we

Table 1 Cut-off distances between oxygen atoms, $R_{\text{OO}}^{(c)}$ and between oxygen and hydrogen atoms, $R_{\text{OH}}^{(c)}$, and O–H···O angle $\phi^{(c)}$, used in our geometrical definition of a hydrogen bond for pure water, water–water pair and water–DMSO pair in 1DMSO : 2H₂O (Their determination is explained in ref. 8 and 18)

	$R_{\text{OO}}^{(c)}/\text{\AA}$	$R_{\text{OH}}^{(c)}/\text{\AA}$	$\phi^{(c)}/\text{degrees}$
pure water	3.5	2.45	30
water–water pair in the mixture	3.5	2.45	30
water–DMSO pair in the mixture	3.2	2.40	30

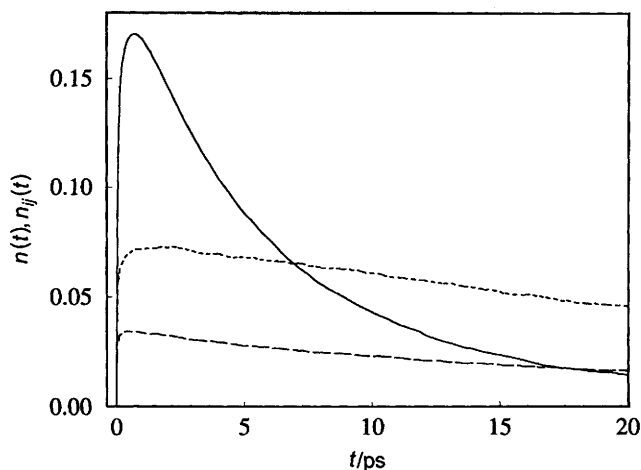


Fig. 2 Populations $n(t)$, eqn. (5), for pure water (solid line), $n_{11}(t)$ for 11 pair in 1DMSO : 2H₂O mixture (dotted line), and $n_{12}(t)$ for 12 pair in the mixture (dashed line)

derive the small time limit of $k(t)$, immediately following the transient time:

$$k(t) \approx k \exp[-(k + k')t] \quad (7)$$

Finding the longest straight line we can draw through the data on Fig. 1(inset panel), we estimate (within the statistical uncertainties) the initial slope and extract k and k' (Table 1). It is important to note that the same values for k and k' , which we obtain from the short time analysis [eqn. (7)] also optimize the agreement between eqn. (6) and simulation results in the range of 1–20 ps.⁵

Bond making rate constant k' is only 30–40% bigger than bond breaking rate constant, k . That means that in the simulation, the free energy of the bonded state is not much lower than that of unbonded nearest neighbour. In the unbonded state, the bond between the tagged pair of molecules no longer exists. Instead, these molecules are now bonded to other nearby partners. In the bond broken state, bonded water molecules have simply switched allegiances. The average frequency of switching allegiance is $k + k'$, which is 1.7 ps^{-1} in the simulation model.⁵

We have thus confirmed and quantified what Stillinger wrote more than 15 years ago: ‘... the hydrogen-bond network has a local preference for tetrahedral geometry, but it contains a large proportion of strained and broken bonds. These strained bonds appear to play a fundamental role in kinetic properties, because their presence enhances prospects for molecules to switch allegiances, trading a bond here for one there and thus altering the network topology’.¹⁹ By drawing only three water molecules for the sake of simplicity, and monitoring the bond between the tagged pair of molecules 1 and 2, the picture that emerges from our calculations⁵ is sketched schematically below (Fig. 3).

According to Fig. 3, molecule 1 was not a nearest neighbour to molecule 3 at time zero (I). All three molecules were in the preferred tetrahedral arrangement. Every once in a while molecule 3, which carries an empty hydrogen-bond site, moves closer to molecule 1 (II). Transition state (TS), a state that must be visited during the passage from one stable state to another, occurs because fluctuations in the environment from perfectly ordered state make an empty hydrogen bonding site accessible. The network of hydrogen bonds is bent and strained. A correlated fluctuation for bond breaking to happen is not required.⁶ There is a sufficient concentration of this necessary disorder present on average, providing the opportunity for bond breaking by a switch of allegiance (III). After the switch, the strained network relaxes and pulls molecules 1 and 2

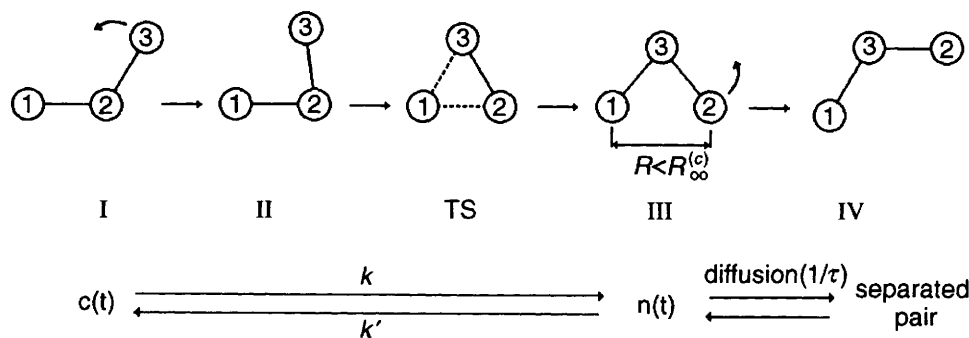


Fig. 3 Mechanism and kinetics of water pair dissociation. Circles represent three hydrogen-bonded (solid lines) water molecules. The dashed line is used in representing the situation where bonds between molecules 1 and 2, and between 1 and 3, are equally likely. Through computer graphics visualization, we have noted that the formation of a new hydrogen bond tends to occur between two water molecules that first have a third water as a common hydrogen-bonded neighbour. The equation below the schematic picture denotes the corresponding populations and relaxation times that are measured in molecular dynamics.

apart, so that they are no longer nearest neighbours. Again, the three molecules find themselves in a preferred tetrahedral arrangement, but this time with molecules 1 and 3 as nearest neighbours (IV).

To the extent that $n(t)$ is non-zero, the two tagged molecules 1 and 2 are no longer bonded to each other but remain nearest neighbours. The population $n(t)$ is therefore a measure of local strain in the hydrogen-bond network. $n(t)$ relaxes not only by conversion back to the bonded state, but also by diffusion. If this diffusion were to occur slowly enough, the sum of $c(t) + n(t)$, which represents the probability that initially bonded pairs of molecules stay nearest neighbours at time t , would appear to be a constant. The separate populations, $c(t)$ and $n(t)$, would each change by interconversion only, relaxing as single exponentials. We can estimate the relevant timescale of diffusion in terms of the elementary diffusion time, τ , *i.e.* the average time it takes for a molecule to diffuse from the domain (of width a) in which a bond with another tagged molecule can exist. In the parlance of ref. 20, τ represents the mean first passage time in an escaping process. It can be approximated by the average diffusion time (averaged over initial positions) from a sphere of radius a , $\tau \approx a^2/15D$. The self diffusion constant D is larger than 10^{-5} cm^2 , and a is less than *ca.* 1.5 Å. These numbers suggest that τ is less than 1 ps for water at standard conditions, a value that is comparable to $1/k$ and $1/k'$. And indeed, the diffusion model for hydrogen-bond kinetics, developed in ref. 5, qualitatively describes our simulation results for two independent correlation functions, *i.e.* $k(t)$ and $k_{\text{in}}(t)$ for liquid water, with the value of $\tau = 0.4[1 \pm 0.25]\text{ps}$.

While the kinetics in the first coordination shell has been established to be very simple [eqn. (6)], relaxation of $n(t)$ by diffusion occurs through a continuum of timescales. We can estimate the degree to which diffusion is significant and we have done so elsewhere.⁵ Most importantly, however, our analysis establishes the existence of well defined rate constants, k and k' , and their connection to microscopic correlation functions [eqn. (6)]. This connection can be used in general to analyse the dynamics of other hydrogen-bonded liquids. In the next section we use it to analyse the kinetics of hydrogen bonds in concentrated aqueous solutions of DMSO. In this case, we are dealing with two distinct types of hydrogen bonds corresponding to water–water (11), and water–DMSO (12) pairs. Here, the quantities that appear in eqn. (1)–(7) refer to a specified type of bond which will be denoted by subscripts (ij) = (11) or (12).

3 Hydrogen-bond kinetics in water–DMSO mixtures

In our earlier work, we studied the water–DMSO system by neutron diffraction with H/D isotope substitution,^{9,21} by computer simulation,^{8,9} and by theoretical modeling.^{22,23} In most of our investigations, the concentration of 1DMSO : 2H₂O was used, since this concentration corresponds to extrema in several thermodynamic^{24,25} and dielectric²⁶ properties, and also, at this high concentration, all water molecules are in close proximity to a DMSO molecule and any significant effect on water structure should be readily observable. As a result of these investigations it is now much clearer what happens when DMSO and water mix. In spite of big differences between molecular geometries of DMSO and water, even at high concentration, DMSO fits rather well into the structure of water, with only minor changes in the local coordination of water molecules. Water readily forms hydrogen bonds with an oxygen on DMSO, but can also rather easily form hydrogen-bonded cages around the hydrophobic methyl groups of DMSO.⁹ 3D histogram extracted from neutron diffraction data of the distribution of water molecules around DMSO molecule in solution points to accumulation of water around both the oxygen atom of DMSO and around the methyl groups of DMSO.²⁷

Let us now consider dynamical consequences of these structural effects. Water near the hydrophobic groups has less opportunity to make hydrogen bonds. Water molecules that are hydrogen bonded to an oxygen atom on DMSO tend to stay in that bond, because water–DMSO hydrogen bond is stronger than water–water hydrogen bond.^{22,25,28} Clearly, the environment of an average water molecule in the mixture contains more confined regions and therefore fewer accessible hydrogen-bond sites. Therefore, the likelihood of fluctuations in the hydrogen-bond network that can lead to hydrogen-bond breaking and to switching allegiance is lower in the mixture than it is in pure water. Thus, we should expect slowing down of water bond dynamics in the presence of DMSO. Functions $k_{ij}(t)$ and $n_{ij}(t)$ computed for the water–water pair in the mixture (from now on denoted as 11 pair), and water–DMSO pair in the mixture (12 pair), presented in Fig. 2 and 4, confirm this expectation.

3.1 Potentials and method

The interactions between water and DMSO molecules were assumed to be composed of pairwise additive potential functions between atomic sites. For water–water interactions we used the rigid SPC model.¹⁶ For DMSO–DMSO interactions, the P2 potential developed in our earlier work,^{8,29} was used. For water–DMSO interactions, we used Lorentz–Berthelot combining rules.⁸ No parameter optimization was carried out for the mixture, once the parameters for pure components have been determined. Classical molecular dynamics simulation was performed on 162 H₂O + 88 DMSO molecules at 300 K, and at the experimental density for the mixture.²⁵ The analysis of dynamical results was carried out on 20 consecutive trajectories, performed in the microcanonical ensemble, each of 10 ps in length, after 200 ps were completed in the canonical ensemble. The Nosé–Hoover thermostat was used to control the temperature for the 200 ps portion. Equations of motion were integrated using a velocity predictor–corrector method with a time step of 1 fs. Time derivatives of the hydrogen-bond correlation functions were calculated each time step. Periodic boundary conditions were used together with the minimum image convention for non-Coulombic interactions. Ewald summation was applied to evaluate the long-range Coulombic forces.¹⁷

4 Results

According to time evolution of $n_{ij}(t)$ for the 11 and 12 pairs in the mixture in comparison with $n(t)$ for pure water (Fig. 2), breaking of a hydrogen bond involves less temporal strain in the mixture than it does in pure water, because the mixture is, on average, more

strained than pure water. The temporal strain, however, relaxes more slowly than it does in water (in terms of absolute times) since the mixture is more constrained and tighter.

Reactive flux correlation functions computed for the 11 and 12 pairs in the mixture $k_{ij}(t)$ show (Fig. 4) a rapid transient decay to values more than an order of magnitude below its initial value. The inset panel shows that the transient period in the mixture is over within 0.5 ps. Reactive flux functions do not show a typical plateau that would be found if we would be dealing with a single elementary process. Slopes of logarithms of $k_{ij}(t)$ for both the 11 and 12 pairs increase monotonically with time. The conclusions that we draw from these calculations are significantly different than those we obtained from 20 times shorter preliminary runs.⁸ The reason for the ever changing slope of $\ln k_{ij}(t)$ is diffusion, as we discussed in Section 2. The self-diffusion constant for water in 1DMSO : 2H₂O mixture is *ca.* three times less than the corresponding value in pure water.³⁰ The elementary diffusion times τ_{ij} , which are expected to scale as $1/D$, should therefore be *ca.* 1.5 ps. Note that by using the diffusion model for hydrogen-bond kinetics, developed in ref. 5, the best fit (not shown in this work) to molecular dynamics results for two independent correlation functions, $k_{ij}(t)$ and $n_{ij}(t)$, at longer times is obtained with $\tau_{ij} \approx 1\text{--}1.5$ ps. These results will be presented elsewhere. Here we concentrate on determining rate constants for the 11 and 12 pairs in the mixture.

In the previous section, we discussed the formalism where we eliminate the effect of diffusion to extract rate constants for the breaking and making of hydrogen bonds, k and k' , eqn. (7). We use this generally applicable procedure to determine the correspond-

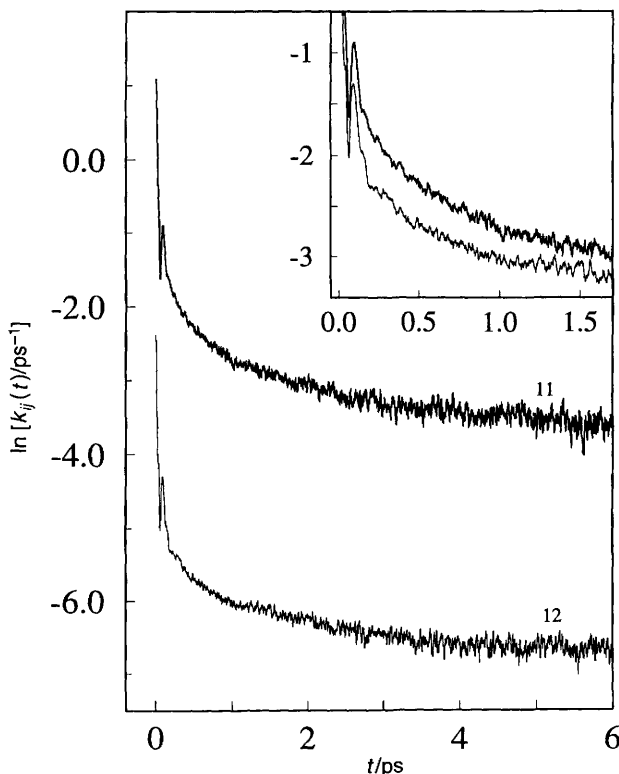


Fig. 4 Reactive flux correlation functions for 11 pair in 1DMSO : 2H₂O mixture (thick line), and 12 pair in the mixture (thin line), sampled over 200 ps of physical time. The inset panel shows portions of trajectories, from which k_{ij} and k'_{ij} were evaluated according to eqn. (7). In the main figure, $\ln k_{12}(t)$ has been shifted down by 3.

Table 2 Rate constants for breaking and making hydrogen bonds, k and k' , determined from eqn. (7), the corresponding TST estimates, k_{TST} , and transmission coefficients, κ [eqn.(3)]

	k/ps^{-1}	k'/ps^{-1}	$k_{\text{TST}}/\text{ps}^{-1}$	κ
water	0.7 (1 \pm 0.10)	1.0 (1 \pm 0.20)	5.1 (1 \pm 0.01)	0.14 (1 \pm 0.11)
11 pair	0.2 (1 \pm 0.30)	1.0 (1 \pm 0.35)	3.2 (1 \pm 0.15)	0.06 (1 \pm 0.45)
12 pair	0.1 (1 \pm 0.30)	0.8 (1 \pm 0.30)	2.1 (1 \pm 0.15)	0.05 (1 \pm 0.45)

ing rate constants, k_{ij} and k'_{ij} in the mixture. Their values are listed in Table 2. The values for hydrogen-bond breaking constants in the mixture are much smaller than in pure water, while the values for hydrogen-bond making constants remain approximately the same. Switching allegiance (Fig. 3) takes less time if many available sites exist in the neighbourhood. In the mixture, there are fewer neighbours with which a new bond can be formed. It therefore takes longer until an appropriate partner for the formation of a new bond is encountered. The rate of returning to the previous tagged bond (measured in terms of k') appears to be less affected by these differences.

One can see significant deviations from the statistical transition-state approximation for the hydrogen-bond breaking rate constant (Table 2). The values of transmission coefficients, estimated from the ratio of hydrogen-bond breaking constant k , and its transition-state theory approximation k_{TST} , indicate that the dynamical corrections to the statistical TST depend slightly (within a factor of two) upon the concentration and the type of hydrogen bond. The observed differences in κ might however also be due to the fact that we do not identify the optimal transition state, as revealed by low values of κ . And it may well be that all the difference in κ for pure water compared with the mixture case stems from having even less optimal transition states in the mixture, than in pure water. This point deserves further investigation. Note that it is a very difficult task to locate the transition state(s) in complex systems with many degrees of freedom. An efficient stochastic sampling method proposed by Pratt³¹ is currently being applied in our laboratory in order to determine transition states.

From determined rate constants we can estimate the difference in the free energies going from state I to state III (Fig. 3), ΔF_s , i.e. free energies for switching allegiance. According to the detailed balance condition

$$\exp(-\beta\Delta F_s) = k/k' \quad (8)$$

where β denotes the inverse of Boltzmann constant times the absolute temperature. In the mixture, the ratio k/k' is replaced by the ratio of corresponding rate constants for the pair under consideration. The values of ΔF_s for pure water, the 11 and the 12 pair in the mixture, are presented in Table 3.

From molecular dynamics data for pure water we also estimate the activation free energy at the apparent transition state, ΔF^*

$$\exp(-\beta\Delta F^*) = P_{\text{TS}}/P_{\text{SS}} \quad (9)$$

where P_{TS} is the probability for being at the transition state (TS), which is the ratio between the time the TS is visited and the total time of the simulation, and P_{SS} is the probability for being at a stable state, i.e. hydrogen bonded. Note, however, that we do not know the optimal choice of the transition state, TS. This leads to an uncertainty in our estimate for P_{TS} which is somewhat bigger than at the true TS. The optimization of transition states should therefore lead to a value of ΔF^* higher than the value listed in Table 3. Planned studies of temperature dependence for $\exp(-\beta\Delta F^*)$, eqn. (9), will determine the activation energy ΔE^* for water from simulation. This will allow an interesting comparison with experimental values for ΔE^* , estimated from the Rayleigh scattering³² and quasi-elastic incoherent neutron scattering³³ experiments.

Table 3 Free energies for switching allegiance, estimated from eqn. (8), ΔF_s , and activation free energies at the transition state, estimated from eqn. (9) and (11), ΔF^* , for water, 11 and 12 pairs in the mixture

	$\Delta F_s/\text{kJ mol}^{-1}$	$\Delta F^*/\text{kJ mol}^{-1}$
water	0.9 (1 ± 0.50)	13.4 (1 ± 0.02)
11 pair	4 (1 ± 0.30)	16.5 (1 ± 0.07)
12 pair	5 (1 ± 0.25)	18.5 (1 ± 0.07)

Errors in ΔF_s , ΔF_{11}^* , and ΔF_{12}^* , were estimated from errors in rate constants, k and k' . Error in ΔF^* for pure water was estimated from differences between the results for various length of trajectories.

The formulation for the rate constant¹⁴ partially includes the influence of the condensed phase environment through the free energy of activation, ΔF^* , as well as the effect of dynamics at or near the transition state:

$$k \approx \kappa \exp(-\beta \Delta F^*) \quad (10)$$

If we, in the first approximation, assume that the dynamical features which are manifested in the value of the transmission coefficient κ do not change from one system to the other, we can attribute all the changes to a statistical effect through ΔF^* . Therefore, we can estimate the free energies of activation for the 11 and 12 pairs from the ratio of the values of bond breaking constants of the 11 and 12 pairs *vs.* the corresponding value in pure water:

$$\begin{aligned} k_{11}/k &= \exp[-\beta(\Delta F_{11}^* - \Delta F^*)] \\ k_{12}/k &= \exp[-\beta(\Delta F_{12}^* - \Delta F^*)] \end{aligned} \quad (11)$$

The transition state occurs due to the fluctuations in the hydrogen-bond network that make an empty hydrogen-bond site accessible. The probability for finding such an empty site for the 11 pair in the mixture is lower compared with pure water, as the 11 pair in the mixture is partly surrounded by bulky hydrophobic methyl groups on DMSO. The activation free energy for water in the mixture is therefore higher than in pure water. The increase in ΔF_{11}^* of *ca.* 3 kJ mol⁻¹ is due to entropic effects. The same consideration applies to the 12 pair, however, an additional energetic effect is also revealed. A larger increase of *ca.* 5 kJ mol⁻¹ in ΔF_{12}^* is consistent with earlier observations that the energy of the hydrogen bond for the 12 pair is stronger than for the 11 pair.^{22,25,28} It would, of course, be interesting to consider separate estimations for activation energies, ΔE^* , and activation entropies, ΔS^* . Studying the temperature dependence of $k(t)$, needed for these calculations, is left for future investigation. Also, up to this point, our analysis of the effect of hydrophobicity on hydrogen-bond dynamics has been based on the net effect of adding DMSO to water. This, of course, is what is done in real experiments. With simulation, more can be done, such as decomposing reactive flux correlation functions according to hydrogen-bond propinquity to methyl groups.

We conclude the discussion of our results by emphasizing that in the case of the 11 and 12 pair in the mixture, the hydrogen-bond lifetimes, $1/k_{ij}$, are much larger than the hydrogen bond deadtimes, $1/k'_{ij}$, and the elementary diffusion times, τ_{ij} . These results could imply that we have a rate-limiting step in the dynamics of hydrogen bonds in the mixture case. Coupling between hydrogen-bond dynamics and diffusion, however, pre-

vents the separation in timescales and concomitant monoexponential kinetics. As already pointed out, the experimentally determined diffusion coefficient for water in 1DMSO : 2H₂O mixture is *ca.* 3 times smaller than the corresponding value in water.³⁰ Computed bond-breaking constants are between *ca.* 4 and *ca.* 7 times smaller than in pure water. Therefore, in the case of the mixture, the time allowed in a practical computer experiment covers only a part of the time interval in which relevant dynamics occurs. k_{ij} and $n_{ij}(t)$ in the mixture are both essentially smaller than in pure water, therefore $k_{ij}c_{ij}(t)$ remains comparable to $k'_{ij}n_{ij}(t)$ and we cannot neglect the second term in eqn. (6).

Finally, we would like to spur some discussion about how our model might be experimentally verified, and what its implications are for measurements and interpretations. We believe that our phenomenological model can be applied to interpret incoherent neutron scattering³⁵ and perhaps transient vibrational spectroscopy.³⁶ Experimental verification of the model will, however, require coordinated application of two different techniques, because $c(t)$ and $n(t)$ are independent functions that vary, at least in the case of pure water, on the same timescale.

The random jump diffusion model has been used by experimentalists to determine the residence time, *i.e.* the characteristic time between diffusive jumps of a water molecule, from quasi-elastic neutron scattering (QENS).^{34,36} It is estimated to be *ca.* 2 ps at room temperature. This time might be compared with the characteristic residence time from our model, that is the average time a molecule spends in a domain in which a bond with another molecule can exist: $1/k + \tau \approx 1.8$ ps.

As yet no rigorous way of deducing hydrogen-bond lifetimes from experimental measurements has been developed. Problems come from the fact that the experimental techniques are sensitive to residence time. In a liquid where hydrogen bonds lead to the formation of dimers, like formic acid, the residence time and the hydrogen-bond lifetime are not very different. In situations where several hydrogen bonds are involved in the coordination shell of a molecule, *e.g.* liquid water, the residence time is larger than the hydrogen-bond lifetime. For water, some attempts are made to obtain an *indirect* determination of the hydrogen-bond lifetime by associating the hydrogen-bond lifetime with a molecular motion related to the breaking of the bond. The same assumption, namely that the mechanism for hydrogen-bond breaking is due to large amplitude librational motions, is made in the interpretation of both depolarized light scattering (DLS)³² and QENS.³⁴ The very low frequency component in the DLS spectrum of liquid water was attributed to the hydrogen-bond making/breaking process. The hydrogen-bond lifetime as estimated from DLS for room temperature water is 0.6 ps.³² This time might correspond to the time needed to switch allegiance in our model, *e.g.* $1/(k + k') = 0.6$ ps. QENS, on the other hand, measures translational diffusion, rotational movements and hydrogen jumps corresponding to the breakage of a bond. Separation of these different contributions is, however, ambiguous. According to our model, which agrees with molecular dynamics calculations, there is a strong coupling between translational and rotational motions for water at room temperature. We hope that the extension of the model will lead to a more reasonable expression to interpret QENS data.

For the mixture water–DMSO, no QENS measurements have yet been performed. We believe that there are several advantages in the interpretation of the data in the mixture case. First, our model predicts $1/k_{11} + \tau_{11} \approx 6$ ps, and $1/k'_{12} + \tau_{12} \approx 11$ ps for the characteristic residence times for the 11 and 12 pairs in the mixtures. In this system the residence times almost coincide with hydrogen-bond lifetimes estimated from the inverse values of the corresponding hydrogen-bond breaking constants, *i.e.* *ca.* 5 ps and *ca.* 10 ps. Further, a selective deuteration of the system should allow a better attribution of the components of the central quasielastic line of QENS to specific molecular movements of the protons of water and DMSO. We hope to report on such experiments in the future.

I am grateful to David Chandler for many enlightening conversations, suggestions, and for critical reading of the manuscript. Discussions and correspondence with José Teixeira about relevant experimental techniques are appreciated. This work is supported by the U.S. ONR.

References

- 1 *Hydrogen-Bonded Liquids*, ed. J. C. Dore and J. Teixeira, Kluwer Academic, Dordrecht, 1990.
- 2 B. M. Ladanyi and M. S. Skaf, *Annu. Rev. Chem.*, 1993, **44**, 335.
- 3 F. H. Stillinger, *Adv. Chem. Phys.*, 1975, **31**, 1.
- 4 I. Ohmine and H. Tanaka, *Chem. Rev.*, 1993, **93**, 2545; A. C. Belch and S. A. Rice, *J. Chem. Phys.*, 1987, **86**, 5676; F. Sciortino, P. H. Poole, H. E. Stanley and S. Havlin, *Phys. Rev. Lett.*, 1990, **64**, 1686.
- 5 A. Luzar and D. Chandler, *Nature (London)*, 1996, **379**, 55.
- 6 A. Luzar and D. Chandler, *Phys. Rev. Lett.*, 1996, **76**, 928.
- 7 A. Geiger, P. Matuschak, J. Schnitker, R. L. Blumberg and H. E. Stanley, *J. Phys. (Paris)*, 1984, **45**, C7; F. Sciortino and S. Fornili, *J. Chem. Phys.*, 1989, **90**, 2786; I. Ohmine, *J. Phys. Chem.*, 1995, **99**, 6767; R. Lamanna, M. Delmelle and S. Cannistraro, *Phys. Rev. E*, 1994, **49**, 2841.
- 8 A. Luzar and D. Chandler, *J. Chem. Phys.*, 1993, **98**, 8160.
- 9 A. K. Soper and A. Luzar, *J. Phys. Chem.*, 1996, **100**, 1357.
- 10 M. Ferrario, M. Haughely, I. R. McDonald and M. L. Klein, *J. Chem. Phys.*, 1990, **93**, 5156.
- 11 D. Chandler, *Introduction to Modern Statistical Mechanics*, Oxford University Press, New York, 1987.
- 12 D. Chandler, *J. Chem. Phys.*, 1978, **68**, 2959; D. Chandler, *J. Stat. Phys.*, 1986, **42**, 49.
- 13 B. J. Berne, in *Multiple Time Scales*, ed. J. U. Brackbill and B. I. Cohen, Academic Press, New York, 1985, p. 419; P. Hanggi, P. Talkner and M. Borkovec, *Rev. Mod. Phys.*, 1990, **62**, 251, and references therein.
- 14 P. Pechukas, *Annu. Rev. Phys. Chem.*, 1981, **32**, 159.
- 15 R. Zwanzig, *Annu. Rev. Phys. Chem.*, 1965, **16**, 67.
- 16 H. J. C. Berendsen, J. P. M. Postma, W. F. van Gunsteren and J. Hermans, in *Intermolecular Forces*, ed. B. Pullman, Riedel, Dordrecht, 1981, p. 331.
- 17 M. P. Alan and D. J. Tildesley, *Computer Simulation of Liquids*, Clarendon, Oxford, 1981.
- 18 A. Luzar and D. Chandler, in *Hydrogen Bond Networks*, ed. M. C. Bellissent-Funel and J. C. Dore, Kluwer Academic, Dordrecht, 1994, p. 239.
- 19 F. H. Stillinger, *Science*, 1980, **209**, 451.
- 20 C. W. Gardiner, *Handbook of Stochastic Methods for Physics, Chemistry and the Natural Science*, Springer, Berlin, 1985.
- 21 A. K. Soper and A. Luzar, *J. Chem. Phys.*, 1992, **97**, 1320.
- 22 A. Luzar, *J. Chem. Phys.*, 1989, **91**, 451.
- 23 A. Luzar, *J. Mol. Liquids*, 1990, **46**, 221.
- 24 M. F. Fox and K. P. Whittingham, *J. Chem. Soc., Faraday Trans.*, 1974, **75**, 1407; J. Kenttamaa and J. Lindberg, *Suom. Kemistil.*, 1960, **B33**, 32; P. Westh, *J. Phys. Chem.*, 1994, **98**, 3222; J. T. W. Lai, F. W. Lau, D. Robb, P. Westh, G. Nielsen, C. Tradum, A. Hvidt and Y. Koga, *J. Solution Chem.*, 1995, **24**, 89.
- 25 J. M. G. Cowie and P. M. Toporowski, *Can. J. Chem.*, 1964, **39**, 2240.
- 26 E. Tommila and A. Pajunen, *Suom. Kemistil.*, 1969, **B41**, 172.
- 27 A. K. Soper, *Faraday Discuss.* 1996, **103**, 41.
- 28 R. Fuchs, G. E. Mcray and J. J. Bloomfield, *J. Am. Chem. Soc.*, 1961, **83**, 4281.
- 29 A. K. Soper, A. Luzar and D. Chandler, *J. Chem. Phys.*, 1993, **99**, 6836.
- 30 K. J. Packer and D. J. Tomlinson, *Trans. Faraday Soc.*, 1971, **67**, 1302.
- 31 L. R. Pratt, *J. Chem. Phys.*, 1986, **85**, 5045.
- 32 O. Conde and J. Teixeira, *J. Phys. (Paris)*, 1983, **44**, 525.
- 33 S. H. Chen, J. Teixeira and R. Niclow, *Phys. Rev. A*, 1982, **26**, 3477.
- 34 J. Teixeira, M. C. Bellissent-Funel, S. H. Chen and A. Dianoux, *J. Phys. Rev. A*, 1985, **31**, 1913.
- 35 S. Bratos and J. C. Leickman, *J. Chem. Phys.*, 1995, **103**, 4887.
- 36 S. H. Chen and J. Teixeira, *Adv. Chem. Phys.*, 1986, **64**, 1; S. H. Chen in ref. 1, p. 289.